NUCLEI FROM "ISLAND OF STABILITY" OF SUPERHEAVY ELEMENTS*

Yu. Oganessian

Flerov Laboratory of Nuclear Reactions, Joint Institute for Nuclear Research
141980 Dubna, Moscow region, Russia

(Received November 7, 2011)

The observation of atomic numbers Z that are 40% larger than that of Bi, the heaviest stable element, is an impressive extension of nuclear survival. Although the super heavy nuclei (SHN) are at the limits of Coulomb stability, shell stabilization lowers the ground-state energy, creates a fission barrier, and thereby enables the SHN to exist. The fundamentals of the modern theory concerning the mass limits of nuclear matter have been experimentally verified.

DOI:10.5506/APhysPolB.43.167
PACS numbers: 27.90.+b, 23.60.+e

1. Introduction

A fundamental outcome of modern nuclear microscopic theory is the prediction of the islands of stability in the region of hypothetical superheavy elements. One important consequence of these calculations [1,2,3,4,5,6,7,8] was the disclosure of a significant gap in the spectrum of low lying levels in the region of the deformed nuclei around $N = 162$ (deformed shell) and of the hypothetical superheavy nuclei, *viz.* of a new (following $N = 126$) closed spherical neutron shell $N = 184$. And finally, at further and quite significant increase of the deformation arising in fission, *the shell effects continued to play an important role* in defining the potential energy and the nuclear inertial masses. New shells push far away the limits of nuclear masses and extend the region of existing heavy nuclei (and chemical elements) at least as far as $Z \sim 120$ and even more.

* Presented at the XXXII Mazurian Lakes Conference on Physics, Piaski, Poland, September 11–18, 2011.

2. Reactions of synthesis

For the synthesis of superheavy nuclei with $Z = 112$–118 with large neutron excess, we chose the fusion reactions: ^{238}U, ^{237}Np, ^{242,244}Pu, ^{243}Am, ^{245,248}Cm, ^{249}Cf + ^{48}Ca, which are characterized by evaporation residues with a maximal number of neutrons [9].

Until now, for the synthesis of all heavy nuclei with $Z = 107$–112, fusion reactions of the magic nuclei ^{208}Pb and ^{209}Bi with a massive projectile ($A_P \geq 50$) were used [10]. In this kind of reactions, the compound nucleus has an excitation energy about $E_x \approx 12$–15 MeV (cold fusion). The transition to the ground state takes place by the emission of only one neutron and γ-rays [11, 12, 13, 14, 15]. As a result, the survivability of the compound nucleus significantly increases, this being the main advantage of the cold fusion reactions. However, as can be seen from Fig. 1 (a), the production cross section of the evaporation products strongly decreases with increasing of Z_{CN}. This indicates the retarding of fusion, leading to the formation of a compound nucleus.

In reactions such as Actinides + ^{48}Ca at excitation energies $E_x \approx 35$–40 MeV (hot fusion), the survivability of the compound nuclei is significantly lower. The two factors, the formation and survival of compound nuclei, lead to decreasing the cross section for the evaporation residues, formed in the reactions of cold and hot fusion (Fig. 1). However, the restrictions themselves arise because of different reasons.

At fixed mass/charge values of the target (^{208}Pb or ^{209}Bi), the increase of the atomic number of the projectile causes an increase in the Coulomb repulsion along the path of the collective motion of the system from the point of contact to the final configuration of the compound nucleus. For this reason the cross section $\sigma_{1n}(Z_{CN})$ will strongly decrease with increasing the atomic number of the compound nucleus (see Fig. 1 (a)).

For more asymmetric in mass/charge hot fusion reactions, type of Act. + ^{48}Ca, the forces hindering fusion are weaker. The main losses are due to fission of the heavy excited nucleus in the process of its de-excitation by means of neutron evaporation. Generally, the survival probability of the nucleus is determined to a large extent by its fissility, which depends on the height of the fission barrier. It should be noted that in nuclei with $Z > 100$ the height of the fission barrier is practically totally defined by shell corrections to the deformation energy of the nucleus. How fissility of the compound nuclei changes as one goes away from the closed deformed shells $N = 152$ and $N = 162$ is well seen on the lower part of Fig. 1 (b). This is the reason for the strong decrease of the cross sections of hot fusion reactions, which are shown in the upper part of the figure. However, as one approaches the closed neutron shell $N = 184$, the height of the fission barrier of the very

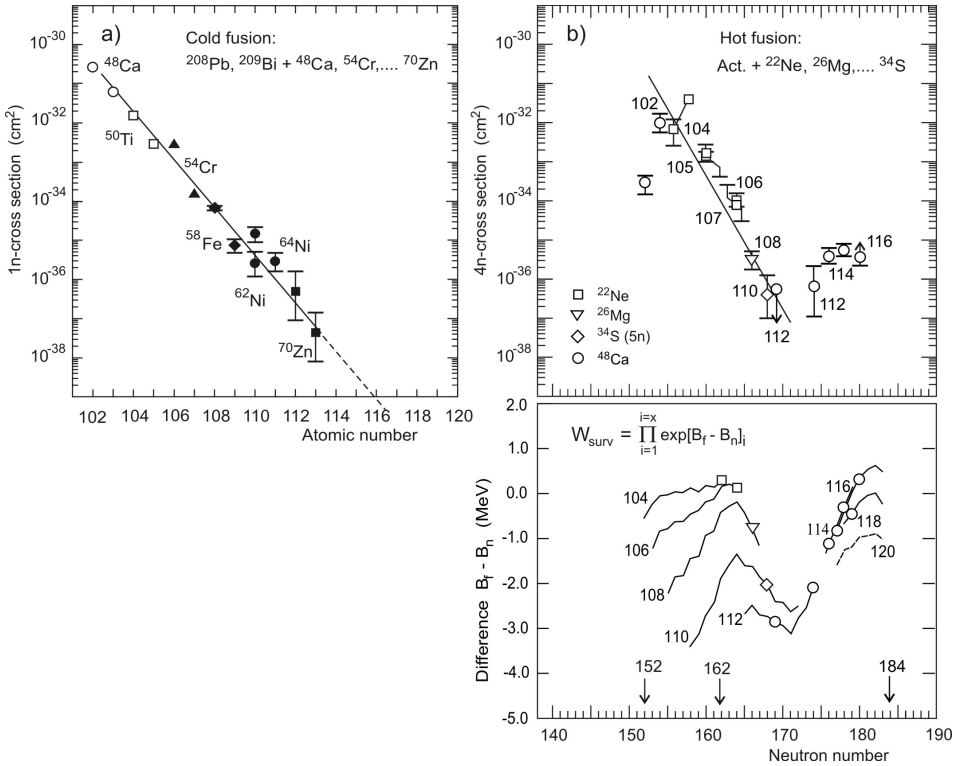

Fig. 1. (a) Production cross section of the $1n$-evaporation channel in cold fusion of the target nuclei ^{208}Pb, ^{209}Bi and ^{50}Ti, ^{54}Cr, ... ^{70}Zn projectiles (Coulomb factor $Z_1\,Z_2 = 1640$–2490). (b) Upper panel: production cross section of the $4n$-evaporation channel in reactions of hot fusion of the actinide target nuclei and ^{22}Ne, ^{26}Mg, ^{34}S-projectiles as a function of the neutron number in the compound nucleus ($Z_1\,Z_2 = 920$–1504). The cross section of the reactions ^{208}Pb and actinide target nuclei with ^{48}Ca-projectiles ($Z_1\,Z_2 = 1640$–1960) shown by circles. Lower panel: calculated values of the difference $(B_n - B_f)$ [23], which determines the survivability of the hot nucleus in the process of its de-excitation by emission of neutrons.

heavy (superheavy) nuclei increases almost by a factor of 2 (calculation) and, as a result of this, the cross sections of the evaporation residues from the Act. + ^{48}Ca reactions also increase (experiment). Such a correlation between the calculated $B_f(Z, N)$ values and the experimental cross sections $\sigma_{xn}(Z, N)$ gives direct evidence of the existence and the strong effect of a neutron shell located at $N \geq 180$.

3. Gas Filled Separator and detectors

The Gas-Filled Recoil Separator (DGFRS) used in the experiments with ^{48}Ca-projectiles is schematically presented in Fig. 2. The typical beam intensity of ^{48}Ca ions at the target was 1.0–1.2 pμA.

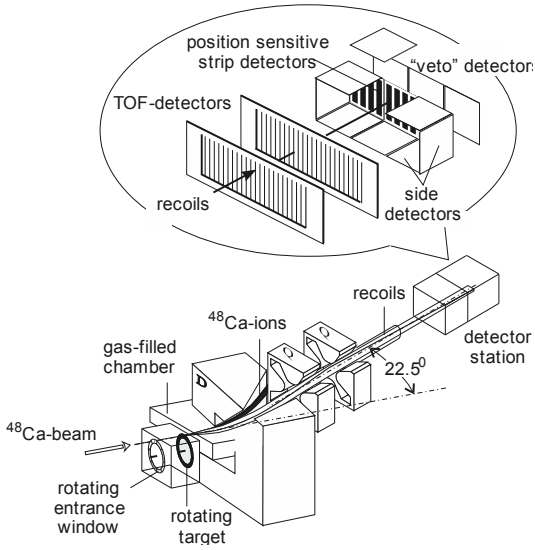

Fig. 2. Layout of the Gas-filled Recoil Separator.

Evaporation residues passing through the separator were implanted in a $4 \times 12\,\mathrm{cm}^2$ semiconductor detector with 12 vertical position-sensitive strips. The detection efficiency of the focal-plane detector array for α-particles is 87% of 4π; for detection of one fission fragment — close to 100%, for two fission fragments — about 40%. The setup allows investigation of nuclei in a range of half-lives from 10^{-5} s to more than 10^5 s.

From the characteristics of the DGFRS, which are given above, it follows that with a ^{48}Ca-beam intensity of 1.2 pμA, 0.35 mg/cm^2 target thickness and a beam dose 5×10^{18} (realized for 200 hours of operation) the observation of one decay event corresponds to the production cross section of about 0.7 pb.

4. Experimental results

For the synthesis of superheavy nuclei at DGFRS, the fusion reactions of ^{48}Ca with target nuclei, the isotopes of Ra, U, Np, Pu, Am, Cm, Bk and Cf (11 isotopes of 8 elements), were used.

4.1. Decay chains

The decay chains of the reaction products obtained with actinide and ^{226}Ra target nuclei are presented in Fig. 3. In the investigations carried out at different ^{48}Ca energies, 48 new nuclides were detected, all of them being evaporation products and their daughter nuclei in the region of $Z = 104 \div 118$ and $A = 266 \div 294$ [16,17,18]. The nuclei produced in cold fusion reactions are also presented in Fig. 3. In cold fusion reactions sequential α-decays of neutron-deficient nuclei led to daughter products in a known nuclear region. The identification of the mass and charge number of a new nuclide is determined here by the decay properties of the known daughter nucleus and by establishing correlations in sequential α-transitions leading to its formation. Evaporation products of the reactions Act. + ^{48}Ca have a larger neutron number; their sequential α-decays take place among unknown nuclei and are terminated by spontaneous fission. In this case some additional measurements are needed.

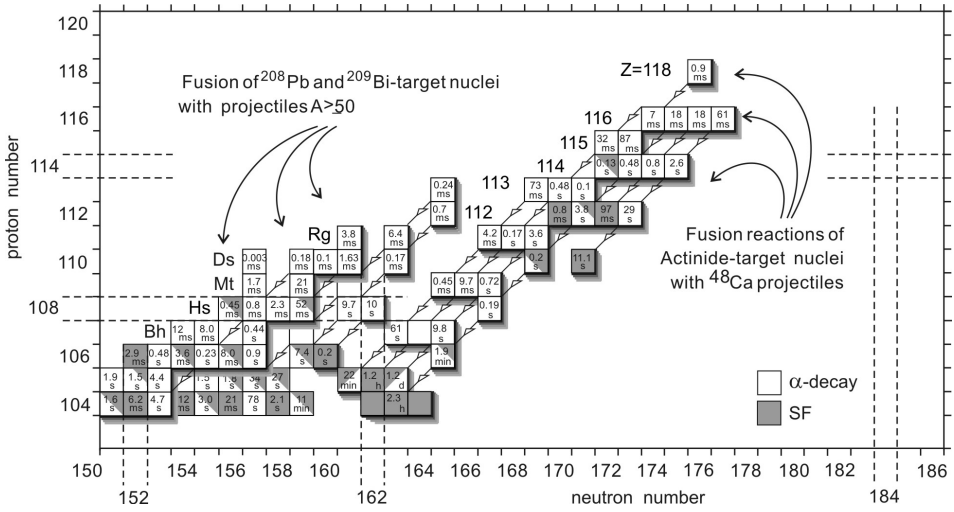

Fig. 3. Chart of the nuclides for $Z \geq 104$. The left and right shaded parts of the graphic present two regions of nuclei, which have been synthesized in cold fusion and in Act. + ^{48}Ca reactions. The nuclei, which are located between these two regions, have been produced in fusion reactions of actinide target nuclei with light projectiles ($A \leq 26$). The half-lives (without experimental errors) for the main decay modes are given in the squares.

The atomic numbers for the odd nuclides (taking into account their long lifetimes) and for all nuclei of its decay chain can be, in principle, determined by means of the chemical isolation of the most long-lived nuclide. Such an experiment was performed including the identification of the odd–odd

SF-nuclide ^{268}Db ($T_{1/2} \approx 32$ h), which terminated the 5-step chain of sequential decay of the mother nucleus ^{288}115, synthesized in the ^{243}Am + ^{48}Ca reaction [19]. Independently, the charge and mass of the nuclides were determined by the excitation functions of the evaporation reaction channels. With this purpose, for all the studied reactions, the production cross sections of a given evaporation product were measured as a function of the energy of the bombarding ion (the excitation energies of the compound nucleus), varying the target isotope (or the mass of the compound nucleus).

4.2. Cross sections

All the above-mentioned data give a consistent picture of the charges and masses of the nuclei, obtained in the experiments with the Act. + ^{48}Ca reactions. The production cross section, the identification, as well as the decay properties of the $Z = 112$, 114 and now 116 were recently confirmed in several independent experiments [20, 21, 22].

In Fig. 4 (a) there are shown fission barrier heights of the heavy nuclei in the region $100 \leq Z \leq 122$ and $158 \leq N \leq 190$ calculated in macro-microscopic model in the version of Möller *et al.* [23]. In the figure there are clearly seen two domains of nuclei with the highest fission barrier height due to the effect of shells $Z = 108$ and $N = 162$ in deformed nuclei and due to much stronger effect of the spherical shells $Z = 114$ and $N = 184$ in superheavy nuclei. Compound nuclei produced in the reactions with ^{48}Ca

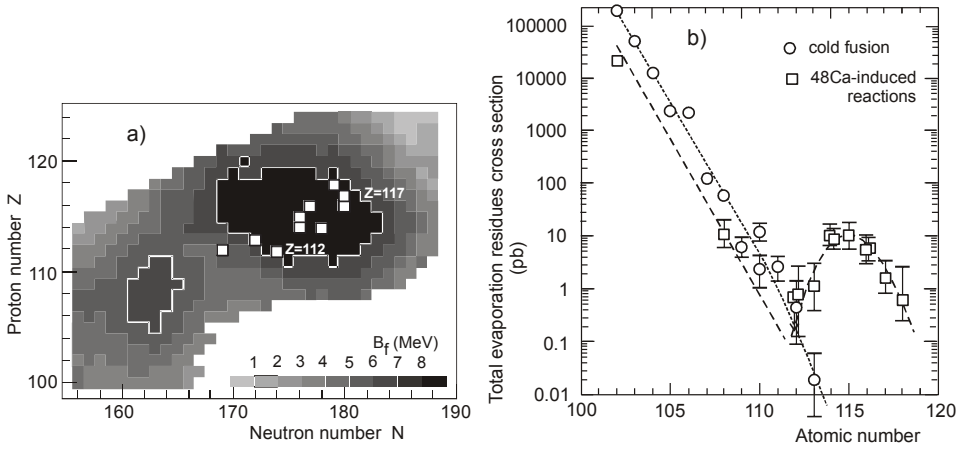

Fig. 4. (a) Fission barrier heights of the trans-fermium nuclei calculated in macro-microscopic model in version [23]. (b) Experimental total evaporation residues cross sections of trans-fermium nuclei produced in cold fusion reactions (^{208}Pb- and ^{209}Bi-based target) and in hot fusion reactions (^{48}Ca-based projectiles).

(white squares in Fig. 4 (a)) are located in the area of the highest calculated fission barrier. This increases survivability of the compound nuclei in the process of their cooling down by emission of neutrons and thus considerably increases the cross section of producing superheavy nuclei in the ground state (Fig. 4 (b)). The correlation we see in the experiments between the formation cross sections of the evaporation residues and the calculated fission barriers shows that the shell effect is also present in the heated nucleus. Maximum cross section of xn-channels of the reaction (generally $x = 3$ and 4) as it is seen in Fig. 4 (b) reach the highest value of about 10 pb for the isotopes with atomic number 114 and 115. A similar picture was expected in macro-microscopic calculations that predict the occurrence of the new spherical shells $Z = 114$ and $N = 184$.

In purely microscopic models of the Hartree–Fock–Bogoliubov (HFB) type or in self-consistent relativistic mean-field calculations (RMF) the closed proton shells shift to $Z = 120$–126; however this effect in production cross sections of the heaviest nuclei up to $Z = 118$ is not observed in our experiments yet. In Fig. 4 (b) it is seen a huge difference in cross sections of production of the heaviest nuclei with $Z \geq 113$ in the cold fusion reactions $^{209}\mathrm{Bi}(^{70}\mathrm{Zn}, n)^{278}113$ and in hot fusion $^{243}\mathrm{Am}(^{48}\mathrm{Ca}, 3n)^{288}115 - \alpha \rightarrow ^{284}113$. The formation cross sections of the isotopes of element 113 in these two reactions differ by a factor of more than 500. While in the cold fusion of the magic nuclei of $^{208}\mathrm{Pb}$ with massive nuclei with $A = 50$–70 the decline of the cross section is caused by hindrance of fusion owing to the increase of the repulsion forces with the increase of mass and charge of ions, in the more asymmetric reactions with $^{48}\mathrm{Ca}$ this effect is weaker. However, in the hot fusion reactions the cross section of producing evaporation residues is very sensitive to the fissionability of the heated and highly fissile compound nuclei. The survivability depends exponentially on the difference between the fission barrier height and the neutron binding energy. In the domain of neutron-rich nuclei owing to the decrease of neutron binding energy and the occurrence of the relatively high fission barrier that is caused by the influence of the spherical shells $Z = 114$ and $N = 184$ the cross section considerably increases that is observed in the experiment.

5. Decay properties of superheavy nuclei

5.1. Alpha-decay

As can be seen from Fig. 3, the odd isotopes of element 112 and all isotopes (even and odd) with $Z \geq 113$ predominantly undergo α-decay. A comparison of the α-decay energies of nuclides with mass $264 \leq A \leq 297$ and atomic number $106 \leq Z \leq 118$, synthesized in the cold fusion reactions

^{208}Pb, ^{209}Bi + ^{58}Fe, ^{64}Ni, ^{70}Zn and in the Act. + ^{48}Ca reactions, are given in Fig. 5. A difference of decay energy Q_α between experiment and theory is present.

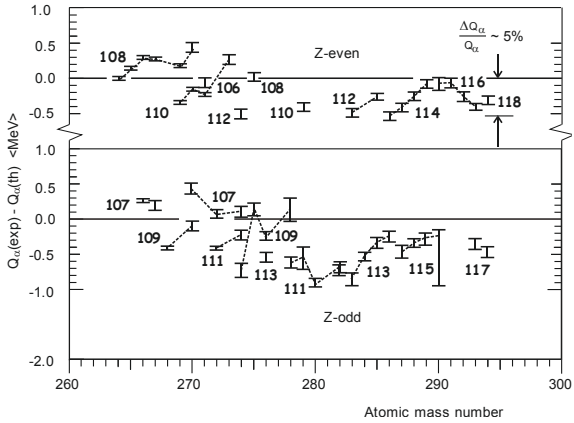

Fig. 5. Comparison of the experimental values of the α-decay energies Q_α(exp) with the calculated within the framework of the macro-microscopic model [24]. The main data belong to nuclei, which have been synthesized in Act. + ^{48}Ca reactions. In the left part of the graph, the data for the light isotopes with Z = 107–113, obtained in cold fusion reactions, are also shown.

The values $\Delta Q_\alpha = Q_\alpha(\text{exp})–Q_\alpha(\text{th})$ are given for the calculation performed in the macro-microscopic model of Ref. [24, 25]. It can be seen that for all even-Z nuclei with Z = 106–118 and A = 271–294, and for nuclei with even as well as with odd number of neutrons, the quantity ΔQ_α does not exceed 0.5 MeV; for odd-Z nuclei: $\Delta Q_\alpha \leq 1.0$ MeV. In both cases, we can assume that there is quite good agreement of theory with experiment, moreover if we keep in mind that the calculation has been performed before obtaining the experimental data. The comparison of Q_α(exp) with the values Q_α(th), calculated within the Skyrme Hartree–Fock–Bogoliubov (HFB) and the Relativistic Mean Field models (RMF), was carried out, too (see [16]). In the HFB model a better agreement is obtained with masses from [26] calculated with 18 parameters. Finally, in the RMF model the agreement between theory and experiment is the least satisfactory. But it cannot be excluded that a better agreement can be achieved in this model also, if a different set of parameters is used. As a whole, the measured values of Q_α(exp) are in agreement with theory, because the model calculations do not claim to be more precise in determining Q_α(th) than 0.4–0.6 MeV.

5.2. Spontaneous fission

For 11 out of the 48 synthesized nuclei spontaneous fission is the predominant mode of decay. In two more nuclei, ^{271}Sg and ^{286}114, spontaneous fission competes with α-decay. For the remaining nuclides spontaneous fission was not observed. The partial SF half-lives of nuclei with $N \geq 163$, produced in fusion reactions with ^{48}Ca, together with the half-lives of SF-nuclides with $N \leq 160$, are shown in Fig. 5. Four isotopes of element 112 with $N = 170$–173 are located in a region, where a steep rise of $T_{\mathrm{SF}}(N)$ is expected. Indeed, in the even–even isotopes ^{282}112 and ^{284}112 the difference of two neutrons increases the partial half-life T_{SF} by two orders of magnitude. The neighbouring odd isotopes ^{283}Cn and ^{285}Cn undergo α-decay. For them, only lower limits of T_{SF} can be determined (shown in the figure). The same refers to the even–even isotopes of element 114: the additional two neutrons in the nucleus ^{286}114 ($T_{\mathrm{SF}} \approx 0.13$ s) lead to increase of the stability relative to spontaneous fission. Such a picture is observed also for odd-Z isotopes: ^{281}Rg ($T_{\mathrm{SF}} \approx 26$ s) and α-emitting odd–odd nucleus ^{282}Rg [18]. It is evident that the rise of stability relative to spontaneous fission is observed for the nuclei, which are by 10–12 neutrons away from the closed neutron shell $N = 184$.

On moving to the nuclei with $Z < 110$ and $N < 170$ the probability for spontaneous fission decreases again when the close deformed shell $N = 162$ is approached. The stabilizing effect of the $N = 162$ shell manifests itself in the properties of the even–even isotopes of Rf, Sg and Hs with $N \leq 160$, which, as seen from Fig. 6, are well described by the mentioned model

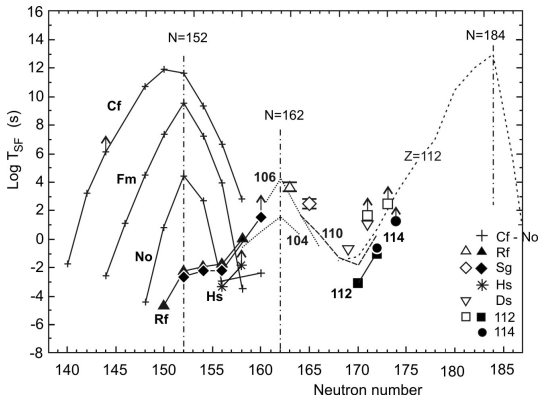

Fig. 6. Partial half-lives for spontaneous fission T_{SF} *versus* N for nuclei with even $Z = 98$–114. Solid symbols and crosses denote even–even, open symbols even–odd nuclei. Solid lines are drawn through the experimental points of even–even nuclei, the dashed lines calculated T_{SF}(th) [8]. Spontaneous fission half-lives of neutron-rich Db-isotopes and of the ^{281}Rg are shown also.

calculations. The odd SF-isotopes with $Z = 104$–110, produced in the ^{48}Ca-induced reactions, are located in the transition region, where the larger the neutron number, the smaller the effect of the $N = 162$ shell. In this region, the $N = 184$ shell comes into effect. Such a behaviour of $T_{SF}(exp)$ as a function of Z and N correlates with the SHE fission barrier heights and has been predicted by all models: MM, HFB and RMF. For the isotopes of element 115, due to the strong hindrances to spontaneous fission of nuclei with odd proton (or/and neutron) number, α-decay predominates as far as the $N = 162$ shell, where, similarly to the previous case, the sequences terminate by spontaneous fission.

6. Half-lives and stability of the heaviest nuclei

In Fig. 7 the half-lives of the isotopes of elements 110–118 are shown.

It can be seen that the stability of the heavy nuclides in the region $N \geq 165$ rises considerably with the increase of N; the increase of the neutron number in the isotopes of elements 110—113 by $\Delta N = 8$ leads to half-lives greater by about 4–5 orders of magnitude. The rise in nuclear stability is observed also for the nuclides with $Z = 114$ and 116, in an interval $\Delta N = 4$. In the macroscopic models, such as the classical liquid drop model (or its modifications), trans-actinide nuclei in the absence of a fission barrier will undergo fission within some 10^{-19} s. The experimental

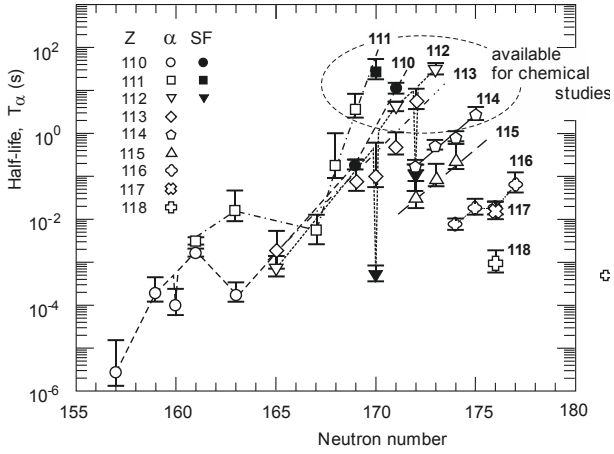

Fig. 7. Half-lives of the nuclei with $Z \geq 110$ (in seconds) *versus* neutron number N. The open symbols denote nuclei undergoing α-decay, the solid symbols "–" spontaneous fission. All nuclides with $N \leq 165$ shown in the figure have been synthesized in cold fusion reactions, nuclei with $N > 165$–in Act. + ^{48}Ca reactions [16,17,18,19]. The curves are drawn through the experimental points to guide the eye.

half-lives, as it follows from Fig. 6, are about 17–19 orders of magnitude longer than expected from this model. Apparently, such a sharp distinction offers evidence of the strong influence of the shell structure of superheavy nuclei on their decay properties. While the relatively high stability in the region of the neutron-deficient deformed nuclei $Z = 110$–112 and $N = 160$–165 can be explained as due to the $N = 162$ shell, the further rise in the region of $N \geq 165$ definitely comes from the effect of another shell, situated at $N > 177$. According to the predictions of all microscopic models, this spherical shell is at $N = 184$ and comes after the lead shell at $N = 126$. We should note the strong effect of the $N = 184$ shell; it manifests itself even in nuclei that are at a distance of 12–14 neutrons (see Fig. 7).

7. Conclusion

Decay properties of the nuclei obtained in Act. + ^{48}Ca reactions show that the basic theoretical concept on the existence of closed shells in the region of the hypothetical superheavy elements and their decisive role in defining the limits of nuclear mass has received its experimental confirmation.

The experiments were carried out at the Flerov Laboratory of Nuclear Reactions (JINR, Dubna) in collaboration with the Lawrence Livermore National Laboratory (LLNL, Livermore), the Oak Ridge National Laboratory (ORNL, Oak-Ridge), the Vanderbilt University (VU, Nashville) and the Research Institute of the Atomic Reactors (RIAR, Dimitrovgrad, Russia); the experiments on the chemical identification of the isotopes ^{268}Db and ^{283}Cn within the collaboration: Paul Scherrer Institute (PSI, Villigen), Department for Chemistry and Biochemistry of the University of Bern, FLNR (Dubna), LLNL (Livermore), Institute of Electronic Technology (IET, Warsaw) with the participation of Dr. M. Hussonois from the Institute of Nuclear Physics (IPN, Orsay).

REFERENCES

[1] M. Brack *et al.*, *Rev. Mod. Phys.* **44**, 320 (1972).
[2] A. Sobiczewski, F.A. Gareev, B.N. Kalinkin, *Phys. Lett.* **22**, 500 (1966).
[3] H. Meldner, *Ark. Fys.* **36**, 593 (1967).
[4] U. Mosel, W. Greiner, *Z. Phys.* **222**, 261 (1969).
[5] P. Möller, J.R. Nix, *J. Phys. G* **20**, 1681 (1994).
[6] W. Greiner, *Int. J. Mod. Phys.* **E5**, (1995).

[7] A. Sobiczewski, *Phys. Part. Nucl.* **25**, 119 (1994).
[8] R. Smolańczuk, J. Skalski, A. Sobiczewski, *Phys. Rev.* **C52**, 1871 (1995).
[9] G.N. Flerov *et al.*, *Nucl. Phys.* **A267**, 359 (1976).
[10] Yu.Ts. Oganessian, *Lect. Notes Phys.* **33**, 221 (1975).
[11] S. Hofmann, *Rep. Prog. Phys.* **61**, 639 (1998).
[12] P. Armbruster, *Annu. Rev. Nucl. Part. Sci.* **35**, 135 (1985).
[13] G. Munzenberg, *Rep. Prog. Phys.* **51**, 57 (1988).
[14] S. Hofmann, G. Munzenberg, *Rev. Mod. Phys.* **72**, 733 (2000).
[15] K. Morita *et al.*, *J. Phys. Soc. Jpn.* **73**, 2593 (2004).
[16] Yu.Ts. Oganessian, *J. Phys. G: Nucl. Part. Phys.* **34**, R165 (2007).
[17] Yu.Ts. Oganessian *et al.*, *Phys. Rev. Lett.* **83**, 3154 (1999); *Phys. Rev.* **C62**, 041604(R) (2000); *Phys. Rev.* **C63**, 011301(R) (2001); *Nucl. Phys.* **A734**, 109 (2004); *Phys. Rev.* **C72**, 034611 (2005); *Phys. Rev.* **C74**, 044602 (2006).
[18] Yu.Ts. Oganessian *et al.*, *Phys. Rev. Lett.* **104**, 142502 (2010).
[19] Yu.Ts. Oganessian *et al.*, *Phys. Rev.* **C72**, 034611 (2005); S.N. Dmitriev *et al.*, *Mendeleev Commun.* **1**, 1 (2005).
[20] S. Hofmann *et al.*, to be published.
[21] L. Stavsetra *et al.*, *Phys. Rev. Lett.* **103**, 132502 (2009).
[22] Ch.E. Dullmann *et al.*, *Phys. Rev. Lett.* **104**, 252701 (2010).
[23] P. Möller *et al.*, *Phys. Rev.* **C79**, 064304 (2009).
[24] I. Muntian, Z. Patyk, A. Sobiczewski, *Acta Phys. Pol. B* **34**, 2073 (2003); *Phys. At. Nucl.* **66**, 1015 (2003).
[25] A. Sobiczewski, *Acta Phys. Pol. B* **41**, 157 (2010).
[26] S. Goriely *et al.*, *Phys. Rev.* **C66**, 024326 (2002).